Group V Phospholipase A_2 Mediates Barrier Disruption of Human Pulmonary Endothelial Cells Caused by LPS *In Vitro*

Steven M. Dudek[1], Nilda M. Muñoz[1], Anjali Desai[1], Christopher M. Osan[1], Angelo Y. Meliton[1], and Alan R. Leff[1]

[1]Section of Pulmonary and Critical Care Medicine, Department of Medicine, University of Chicago, Chicago, Illinois

We examined the functional role of 14-kD secretory group V phospholipase A_2 ($gVPLA_2$) on the barrier function of pulmonary endothelial cells (ECs) after LPS activation *in vitro*. Expression of $gVPLA_2$ was elicited by 20 ng/ml LPS as demonstrated by increased (*1*) mRNA, (*2*) protein content, and (*3*) cell surface expression of $gVPLA_2$ within 4 hours. The effect of LPS on EC barrier function was measured by transendothelial monolayer electrical resistance (TER). LPS increased permeability across EC monolayers at 2–3 hours, and was sustained for 10 hours or more. Blockade of $gVPLA_2$ with mouse monoclonal 3G1 (MCL-3G1) monoclonal antibody directed against $gVPLA_2$ inhibited EC barrier dysfunction elicited by LPS in a time- and concentration-dependent manner; control IgG had no effect on TER. Like LPS, exogenous $gVPLA_2$ caused increased EC permeability in a time- and concentration-dependent manner; neither $gIIaPLA_2$, a close homolog of $gVPLA_2$, nor W31A, an inactive mutant of $gVPLA_2$, caused a decrease in EC TER. Immunofluorescence analysis revealed comparable F-actin stress fiber and intercellular gap formation for ECs treated with either $gVPLA_2$ or LPS. Treatment with $gVPLA_2$ disrupted vascular endothelial–cadherin junctional complexes on ECs. Coincubation of ECs with MCL-3G1 substantially attenuated the structural changes caused by $gVPLA_2$ or LPS. We demonstrate that (*1*) $gVPLA_2$ is constitutively expressed in ECs and is up-regulated after LPS activation, (*2*) endogenously secreted $gVPLA_2$ from ECs after LPS increases EC permeability through F-actin and junctional complex rearrangement, and (*3*) inhibition of endogenous $gVPLA_2$ from ECs is sufficient to block disruption of the EC barrier function after LPS *in vitro*.

Keywords: phospholipase A_2; vascular permeability; cytoskeleton; actin; acute lung injury

The acute lung injury (ALI)/acute respiratory distress syndrome (ARDS) is a devastating consequence of systemic inflammatory conditions, such as sepsis, afflicting an estimated 200,000 people per year in the United States, with 75,000 deaths (1). Despite advances in ventilator management and supportive care (2), the mortality rate for ALI/ARDS remains unacceptably high (>25%) (3). No specific therapy targeted at the underlying pathophysiology of ALI/ARDS is yet available (4, 5).

The hallmark of ALI is disruption of the alveolar–vascular barrier, resulting in vascular leakage of fluid, protein, and cells into the airspaces of the lung, with subsequent severe hypoxia causing respiratory compromise. Inflammatory disruption of the lung vascular endothelial cell (EC) barrier is an essential early step in the pathogenesis of ALI/ARDS, leading to pulmonary edema and subsequent respiratory compromise (5, 6). EC barrier function is primarily regulated by the structural arrangement of the complex array of proteins that comprise the EC cytoskeleton in conjunction with junctional complexes (4, 5). The current paradigm of EC barrier regulation suggests that a balance exists between cellular contractile forces and barrier-protective cell–cell and cell–matrix tethering forces (7).

Secretory phospholipase A_2s ($sPLA_2$s) are a family of lipolytic enzymes that catalyze the cleavage of fatty acids from the *sn*-2 position of phospholipids, leading to the generation of free fatty acids and lysophospholipids (8, 9). $sPLA_2$ has been implicated in the pathogenesis of ALI in both animals (10, 11) and humans (12). This includes prior studies demonstrating that increased concentrations of $sPLA_2$ are found in the lungs, bronchoalveolar lavage fluid, and blood of patients, and correspond to the severity of lung injury (13). However, the regulatory role of 14 kD secretory group V PLA_2 ($gVPLA_2$) in barrier disruption remains undefined.

The functional differences between $gVPLA_2$ and its close homolog, $gIIaPLA_2$, have only recently been differentiated (17, 18). $gVPLA_2$ has much higher affinity than $gIIaPLA_2$ for zwitterionic phosphatidylcholine-rich outer plasma membranes, and therefore greater ability to generate free fatty acids and lysophospholipids at these surfaces (14, 15). Therefore, $gVPLA_2$ is a more effective paracrine agent during inflammation, and is better able to augment PMN functions (21, 22), which are recognized as the primary agents in mediating tissue damage during ALI (23, 24).

We recently reported that inhibition of $gVPLA_2$ by mouse monoclonal 3G1 (MCL-3G1), a specific monoclonal antibody (mAb) directed against $gVPLA_2$ (16–18), blocks LPS-induced airway edema, increased bronchoalveolar lavage fluid protein, myeloperoxidase activity, and neutrophil migration that corresponded to decreased transthoracic static compliance in mice (19). In these studies, deletion of the gene encoding $gVPLA_2$ in mice (*pla2 g5*$^{-/-}$ knockout) (20) blocked these pathophysiological changes after LPS challenge (19). These prior data imply that $gVPLA_2$ secretion is a significant first step in the induction of ALI by LPS. However, the mechanism by which $gVPLA_2$ is synthesized and secreted from activated ECs to cause disruption of the endothelial barrier leading to ALI has not been elucidated previously.

The objective of this investigation was to evaluate the hypothesis that LPS causes increased endothelial permeability

CLINICAL RELEVANCE

We conclude that group V phospholipase A_2 ($gVPLA_2$), which is constitutively expressed in human vascular endothelial cells, is up-regulated in autocrine fashion by LPS. $gVPLA_2$ causes progressive and sustained increases in endothelial intercellular permeability, with associated leak of high–molecular weight molecules. Our studies thus provide preliminary evidence for a regulatory role for $gVPLA_2$ in the vascular leak of acute lung injury syndromes

(*Received in original form December 9, 2009 and in final form February 26, 2010*)

This work was supported by National Institutes of Health/National Heart Lung Blood Institute grants R01 HL-88144 (S.M.D.) and HL-85779 (A.R.L.), and by a grant from the GlaxoSmithKline Center of Excellence in Asthma (A.R.L.).

Correspondence and requests for reprints should be addressed to Steven M. Dudek, M.D., Section of Pulmonary & Critical Care Medicine, Department of Medicine, University of Chicago, 5841 South Maryland Avenue, Chicago, IL 60637. E-mail: sdudek@uic.edu

Am J Respir Cell Mol Biol Vol 44. pp 361–368, 2011
Originally Published in Press as DOI: 10.1165/rcmb.2009-0446OC on May 6, 2010
Internet address: www.atsjournals.org

through up-regulation of $gVPLA_2$ synthesis in ECs and subsequent direct effects of $gVPLA_2$ on ECs to produce barrier disruption. For these studies, we used human pulmonary ECs to test our hypotheses, which were derived from prior physiological observations of the murine model of ALI (19). Studies were performed to determine the temporal correspondence between decreased transendothelial monolayer electrical resistance (TER) across the vascular endothelial monolayer and secretion of $gVPLA_2$ caused by LPS. Further studies were performed to demonstrate that (*1*) induction of decreased TER was specific to this 14-kD secretory $gVPLA_2$, and (*2*) F-actin rearrangement and vascular endothelial (VE)–cadherin disruption resulted in EC intercellular gap formation that was $gVPLA_2$ dependent.

Our data demonstrate that $gVPLA_2$ is expressed constitutively in ECs and is up-regulated after LPS activation. We also demonstrate that endogenous secretion of $gVPLA_2$ from ECs caused by LPS activation increases EC permeability through F-actin and junctional complex rearrangement. Specific blockade of $gVPLA_2$ by MCL-3G1, a mAb directed against $gVPLA_2$, is sufficient to inhibit the electrophysiological and morphological changes caused by LPS in human ECs *in vitro*. These data provide possible mechanistic insights into the induction of ALI by LPS, and further establish that $gVPLA_2$ caused autocrine activation of EC disruption to elicit vascular leak.

MATERIALS AND METHODS

Reagents

Recombinant human $gVPLA_2$ protein, $gIIaPLA_2$ protein, and MCL-3G1, a mAb directed against $gVPLA_2$, were purchased from Cayman Chemical (Ann Arbor, MI). Immunofluorescent reagents were Texas red phalloidin (Invitrogen, Carlsbad, CA) and mouse anti–VE-cadherin antibody (Santa Cruz Biotechnology, Santa Cruz, CA). All other reagents (including LPS) were obtained from Sigma-Aldrich Chemical Co. (St. Louis, MO), unless otherwise noted.

Cell Culture

Human pulmonary artery ECs (HPAECs) and human lung microvascular ECs (HLMVECs) were obtained from Lonza (Walkersville, MD), and were cultured according to the manufacturer's instructions, as previously described (21). ECs (passages 6–9) were grown in endothelial growth medium–2 at 37°C in a 5% CO_2 incubator. The medium was changed 1 day before experimentation.

TER

ECs were grown to confluency in polycarbonate wells containing evaporated gold microelectrodes, and TER measurements were performed using an electrical cell-substrate impedance sensing system (Applied Biophysics, Troy, NY), as previously described in detail (22). Experiments were performed as follows. ECs were treated with: (*1*) vehicle control; (*2*) IgG Ab isotype-matched control; (*3*) 20 ng/ml LPS; (*4*) 100 nM-500 nM $gVPLA_2$; (*5*) 100 nM-500 nM $gIIaPLA_2$; or (*6*) 100–500 nM W31A, an inactive mutant of $gVPLA_2$, at different time intervals before TER assay. In separate experiments, ECs were coincubated with MCL-3G1 and LPS or $gVPLA_2$, and TER measurements were performed as described here. TER values from each microelectrode were expressed as normalized resistance, pooled as discrete time points, and plotted versus time as the mean (±SEM).

Dextran Transwell Permeability Assay

A transendothelial permeability assay was performed per manufacturer's instructions using labeled tracer flux across confluent ECs grown on confluent polycarbonate filters (Vascular Permeability Assay Kit; Millipore, Billerica, MA), as previously described (23). Briefly, ECs on Transwell inserts were exposed to 100 nM $gVPLA_2$ or 500 nM $gVPLA_2$ for 1 hour. FITC-labeled dextran (~60 kD) was added to the luminal compartment for an additional 2 hours, and FITC-dextran clearance across the filter to the abluminal compartment was measured by relative fluorescence excitation at 485 nm and emission at 530 nm. Data were expressed as arbitrary fluorescence units.

Immunofluorescence

ECs were grown on gelatinized cover slips before exposure to various conditions, as described for individual experiments. ECs were then fixed in 3.7% formaldehyde for 10 minutes, permeabilized with 0.25% Triton-X100 for 5 minutes, washed in PBS, blocked with 2% BSA in Tris-buffered saline–Tween for 1 hour, and then incubated for 1 hour at room temperature with the primary antibody of interest. After washing, ECs were incubated with the appropriate secondary antibody conjugated to immunofluorescent dyes (or Texas red–conjugated phalloidin for actin staining) for 1 hour at room temperature. Final washing was performed with Tris-buffered saline–Tween, and coverslips were mounted using Prolong Anti-Fade Reagent (Invitrogen) and analyzed using a Nikon Eclipse TE2000 inverted microscope (Melville, NY).

Immunoblotting Analysis

Cultured ECs were stimulated with either vehicle control or 20 ng/ml LPS for 4 hours at 37°C. Treated ECs were subsequently washed with cold Ca^{2+}/Mg-free PBS, and lysed with 0.3% SDS lysis buffer containing protease inhibitors (1 mM EDTA, 1 mM PMSF, 1 mM sodium orthovanadate, 1 mM sodium fluoride, 0.2 TIU/ml aprotinin, 10 μM leupeptin, 5 μM pepstatin A). Sample proteins were separated with 4–15% SDS-PAGE gels (Bio-Rad, Hercules, CA) and transferred onto Immobilion-P PVDF membranes (Millipore). Membranes were then immunoblotted with MCL-3G1 mAb (1:500–1,000, 4°C, overnight), followed by secondary antibodies conjugated to horseradish peroxidase (1:5,000, room temperature, 30 min). Expression of $gVPLA_2$ was detected with enhanced chemiluminescence (Pierce ECL or SuperSignal West Dura; Pierce Biotechnology, Rockford, IL) on Biomax MR film (Kodak, Rochester, NY). Multiple blots were scanned and quantitatively analyzed using ImageQuant software (v5.2; Molecular Dynamics, Piscataway, NJ).

mRNA Expression for $gVPLA_2$

Total RNA was isolated from ECs using TRIzol reagent, per manufacturer's instructions (Life Technology, Rockville, MD). RNA samples were quantified by measuring optical density at 260 nm using the NanoDrop ND 1,000 Spectrophotometer (Thermo Scientific, Wilmington, DE). cDNA was synthesized from 1 μg/ml of total RNA, per the manufacturer's instructions, using the Invitrogen SuperScript III First-Strand Synthesis SuperMix for qRT-PCR kit (cat. no. 11752-050). The primers for $gVPLA_2$ were: sense, 5′-TTGGTTCCTGGCTTGTAGT GTG-3′; and antisense, 5′-TGGGTTGTAGCTCCGTAGGTTT-3′. For 18 s rRNA, the primers used were: sense, 5′-AAACGGCTACCA CATCCAAG-3′; and antisense, 5′-CCTCCAATGGATCCTCGTTA-3′. Semiquantitative RT-PCR was performed using the Bio-Rad My Cycler Thermal Cycler system (Bio-Rad, Hercules, CA) and AmpliTaq Gold(R) DNA Polymerase (cat. no. 4,311,806; Applied Biophysics) using the following PCR conditions: 10 minutes at 93°C, followed by 40 cycles of 30 seconds at 95°C, 45 seconds at 60°C, 50 seconds at 72°C, and 10 minutes at 72°C. PCR products were separated by electrophoresis in a 1.5% agarose gel, and then stained with ethidium bromide.

Analysis of Membrane-Bound $gVPLA_2$ Expression

ECs were cultured to 90% confluence and resuspended in endothelial growth medium–2 (5% FBS) (Lonza). Aliquots of 2×10^5 cells were incubated at 37°C with Hanks' balanced salt solution buffer or 20 ng/ml LPS. The cells were fixed with 1% paraformaldehyde in H_2O, and stored at 4°C. ECs were incubated with 10 μg/ml of mAb directed against $gVPLA_2$ (MCL-3G1; Cayman Chemical) or isotype-matched control IgG1 Ab at 4°C. After 60 minutes, treated ECs were washed twice with Hanks' balanced salt solution plus 0.2% BSA before addition with an excess of FITC-conjugated goat anti-mouse IgG for 45 minutes at 4°C. Final washing was performed to remove the excess Ab before flow cytometric analysis (BD Biosciences, Franklin Lakes, NJ). Fluorescence intensity was determined on at least 10,000 cells from each sample as acquired using FACscan flow cytometry (BD Bioscience). For quantitative evaluation, the $gVPLA_2$ populations

were gated manually, and the percentage gVPLA$_2$-positive cells was determined using CellQuest software (BD Biosciences, Franklin Lakes, NJ). The results were expressed as the mean fluorescence intensity.

Statistical Analysis

Data are expressed as means (±SEM). Statistical analyses among groups were performed using standard Student's *t* test or one-way ANOVA. Statistical analyses between groups were compared by Newman-Keuls test. Statistical significance in all cases was defined at a *P* value less than 0.05.

RESULTS

Expression of gVPLA$_2$ in Human Pulmonary ECs

We first examined the effects of LPS on gVPLA$_2$ expression in cultured ECs. LPS (20 ng/ml) significantly increased gVPLA$_2$ mRNA expression within 1 hour by 42% relative to baseline control levels, which persisted for 4 hours or more (Figure 1A). This concentration of LPS has been shown previously to cause disruption of the EC barrier without inducing cytotoxicity (24). We next quantified the protein content of gVPLA$_2$ in treated ECs. gVPLA$_2$ protein, which is constitutively expressed in unstimulated ECs, was up-regulated 4 hours after treatment with LPS (Figure 1B, inset, representative Western blot). Densitometric analysis demonstrated that LPS increased gVPLA$_2$ protein expression by almost twofold compared with the unstimulated baseline ($P < 0.05$).

To determine if LPS increases surface expression of gVPLA$_2$ on ECs, membrane-bound expression for gVPLA$_2$ was analyzed by flow cytometric analysis (Figure 1C). Surface expression of gVPLA$_2$ caused by LPS increased in a time-dependent manner. gVPLA$_2$ expression was increased significantly above baseline level by 1 hour, and was greatest 2 hours or more after LPS activation. Vehicle control or IgG1, an irrelevant isotype-matched control Ab, had no effect on surface expression of gVPLA$_2$ in ECs. These data demonstrate that human pulmonary ECs constitutively express gVPLA$_2$, that this expression is inducible by LPS over a 4-hour time period, and that pulmonary ECs express gVPLA$_2$ at the outer membrane surface in response to LPS.

Disruption of EC Barrier Function by LPS Is Mediated by gVPLA$_2$

We next determined the effects of LPS on EC barrier regulation *in vitro* by measuring TER of cultured HPAECs grown on gold microelectrodes, a highly sensitive method for obtaining real-time permeability data (21, 25). A representative tracing on timecourse for treated ECs is shown in Figure 2A. A decrease in EC TER (which correlates with increased permeability and disruption of barrier function) was elicited within 2–4 hours after application of LPS, and persisted for over 10 hours. Disruption of the EC barrier corresponded temporally with the increase in EC gVPLA$_2$ protein and surface expression caused by LPS (*see* Figure 1). Blockade of ECs with MCL-3G1, an mAb directed against gVPLA$_2$ (16–18), significantly attenuated barrier disruption caused by LPS. IgG Ab, an isotype-matched control, had no effect on EC TER (Figure 2A).

Composite data from multiple independent experiments demonstrated that TER decreased by approximately 30% after activation of ECs with 20 ng/ml LPS (Figure 2B). Specific blockade of ECs with 25 μg/ml MCL-3G1 given concurrently with LPS significantly attenuated the disruption of barrier function ($P < 0.05$ versus LPS-treated ECs, no MCL-3G1). Control IgG Ab coincubated with LPS had comparable effect with LPS alone in causing disruption of barrier function. Lower concentrations of MCL-3G1 applied concurrently with LPS, or

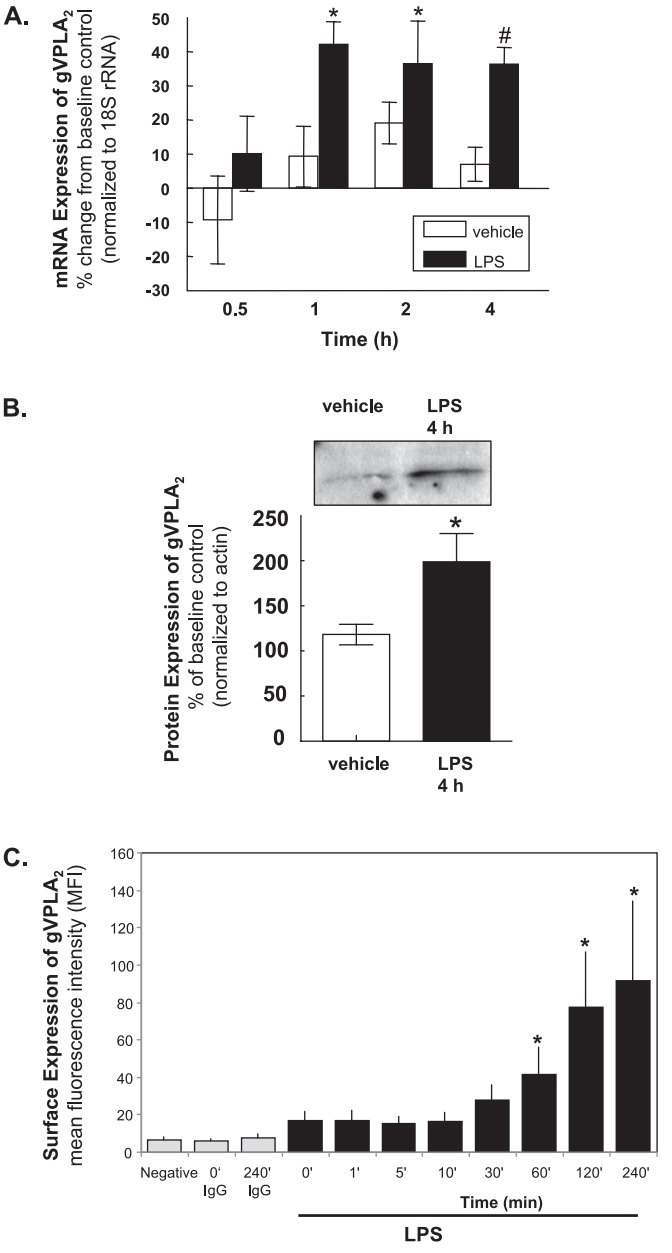

Figure 1. LPS up-regulates group V phospholipase A$_2$ (gVPLA$_2$) in human pulmonary endothelial cells (ECs) *in vitro*. (*A*) mRNA Expression. Human pulmonary artery ECs (HPAECs) were incubated with 20 ng/ml LPS or vehicle control for 0–4 hours, and mRNA expression for gVPLA$_2$ was assessed by semiquantitative PCR, as described in MATERIALS AND METHODS. *Bar graph* represents results of densitometric quantification of multiple independent experiments ($n = 3$–4 per condition; $^*P < 0.05$, $^{\#}P < 0.001$). (*B*) Protein expression. HPAECs were incubated with 20 ng/ml LPS for 4 hours, and gVPLA$_2$ protein expression was assessed by Western blot with mouse monoclonal 3G1 (MCL-3G1) monoclonal antibody (mAb). A representative blot is shown in the *inset*. *Bar graph* represents densitometric quantification from multiple independent experiments ($n = 5$; $^*P < 0.05$). (*C*) Time-related surface expression. Surface expression of gVPLA$_2$ in HPAECs was performed by immunofluorescence flow cytometry, as described in MATERIALS AND METHODS. As indicated along the *x axis*, samples were collected 0–240 minutes after 20 ng/ml LPS stimulation, and then incubated with MCL-3G1 mAb (*black boxes*). Samples incubated with isotype-matched IgG or no antibody (negative) controls are shown for comparison (*gray boxes*). No significant change in mean fluorescence intensity (MFI) was detected until 30 minutes after LPS stimulation, but increased thereafter for 4 hours. Fluorescence intensity was determined on more than 10,000 cells from each sample ($n = 4$ experiments; $^*P < 0.05$).

25 μg/ml MCL-3G1 applied 2–4 hours after LPS, did not significantly inhibit decreased TER caused by LPS (data not shown).

EC Cytoskeletal Rearrangement after LPS Is Mediated by gVPLA$_2$

EC barrier function is primarily regulated by the structural arrangement of the highly complex array of proteins that comprise the EC cytoskeleton (7, 21). The current paradigm of EC barrier regulation suggests that a balance exists between cellular contractile forces and barrier-protective cell–cell and cell–matrix tethering forces (7). Because actin rearrangement is a primary mechanism for EC barrier regulation, we next examined the effects of LPS stimulation on F-actin structure in cultured ECs (Figure 3). Consistent with structural changes known to occur during EC barrier disruption (26), LPS caused formation of F-actin stress fibers and large intercellular gaps in the EC monolayer by 4 hours (*see arrows*), which corresponded to the decreased TER caused by LPS at 4 hours (*see* Figure 2A). Coincubation of LPS with MCL-3G1, an mAb directed against gVPLA$_2$, blocked these effects; this was not the case with control IgG Ab.

Recombinant gVPLA$_2$ Directly Increases EC Permeability

To determine the direct effects of gVPLA$_2$ on EC barrier function, recombinant human gVPLA$_2$ was added to cultured human pulmonary ECs in the TER assay. Exogenous recombinant gVPLA$_2$ increased HPAEC permeability in a concentration-dependent fashion that was sustained for over 5 hours (Figure 4A). Given the well described differential responses of pulmonary macrovascular ECs compared with pulmonary microvascular ECs to various barrier-altering agonists, such as thapsigargin (27) or thrombin (28), we next assessed the effects of gVPLA$_2$ on HLMVECs. Exogenous recombinant gVPLA$_2$ significantly increased HLMVEC permeability in a concentration-dependent fashion, but the magnitude of this barrier disruption was less than that observed in HPAECs (Figure 4B). In further quantitative studies, a Transwell assay using labeled dextran (~60 kD) was employed to determine if gVPLA$_2$ also increased HPAEC permeability to larger particles. Exogenous recombinant gVPLA$_2$ (500 nM) significantly increased HPAEC permeability to dextran as a cumulative measurement after 2 hours of incubation (Figure 4C). In control studies, increased HPAEC permeability caused by gVPLA$_2$ was not replicated by its 14-kD structural homolog, gIIaPLA$_2$ (Figure 5A). There was no decrease in TER after gIIaPLA$_2$ activation, even after 10 hours at the highest concentration used. We also tested the effect of W31A, an inactive mutant of gVPLA$_2$ (29, 30), on the EC TER assay. Like gIIaPLA$_2$, the W31A mutant caused no decrease in TER relative to vehicle control (Figure 5B).

Recombinant gVPLA$_2$ Induces EC F-Actin and VE-Cadherin Rearrangement

To examine the mechanisms by which gVPLA$_2$ disrupts barrier function, we first characterized HPAEC cytoskeletal structure

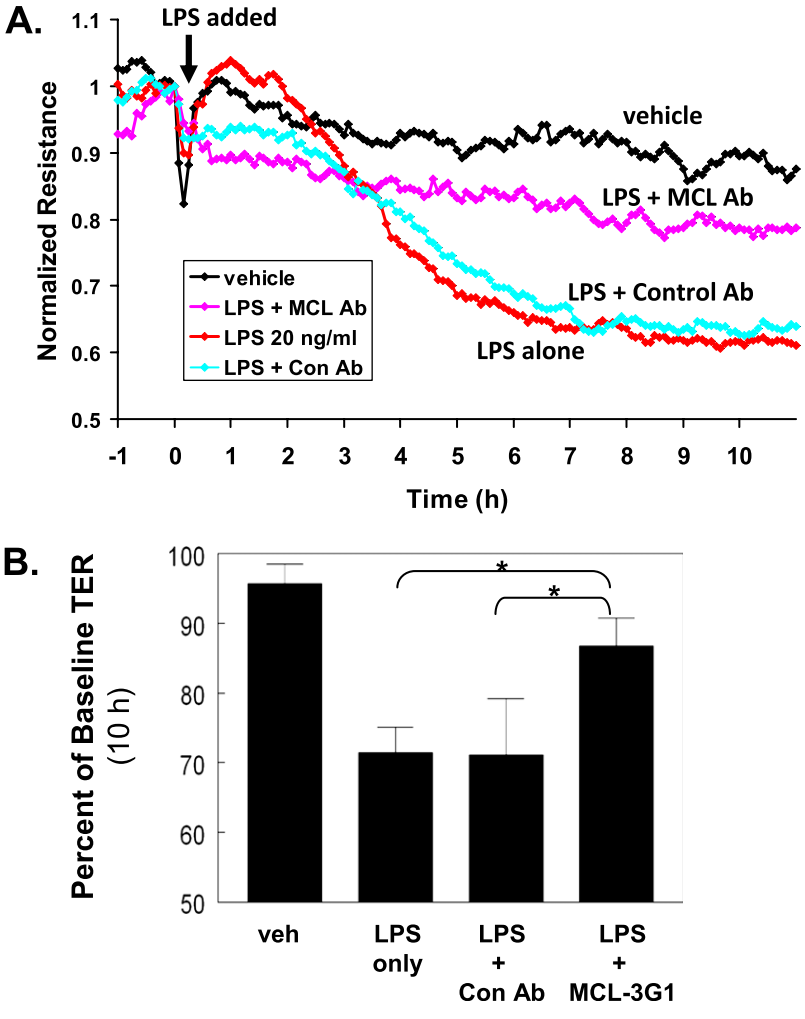

Figure 2. LPS disruption of EC barrier function is mediated by gVPLA$_2$. (*A*) HPAECs were cultured on gold microelectrodes, and real-time transendothelial monolayer electrical resistance (TER) measurements were taken as per MATERIALS AND METHODS. At time 0 (*arrow*), ECs were stimulated with 20 ng/ml LPS (*red line*), vehicle control (*black line*), LPS plus 25 μg/ml MCL-3G1 mAb (*purple line*), or LPS plus 25 μg/ml IgG control Ab (*aqua line*). A representative TER tracing is shown. (*B*) TER data were pooled from multiple independent experiments, and are expressed as percent of vehicle control resistance (TER) at 10 hours of incubation with LPS. MCL-3G1 mAb inhibits the decrease in TER caused by LPS (n = 3–7 per condition; $^*P < 0.05$).

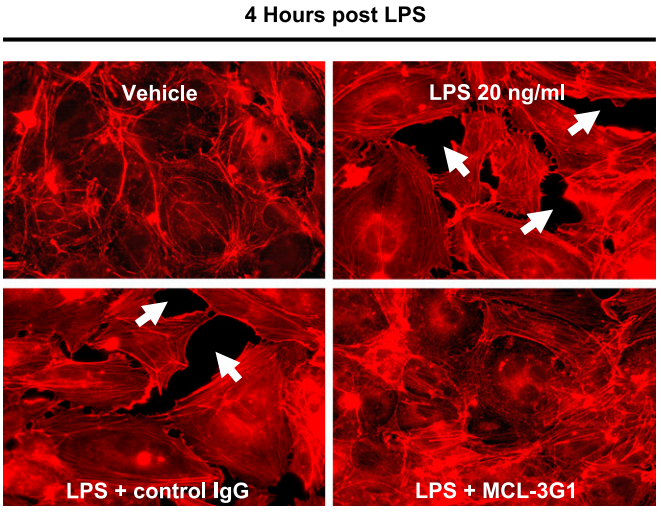

Figure 3. MCL-3G1 mAb attenuates LPS-induced EC gap formation. HPAECs were stimulated with vehicle or 20 ng/ml LPS for 4 hours and stained for F-actin. Parallel LPS-stimulated human ECs were coincubated with MCL-3G1, or control IgG (25 μg/ml). *Arrows* indicate intercellular gaps. *Images* are representative of three independent experiments.

at 5 minutes and at 4 hours by immunofluorescence. As for LPS (Figure 3), recombinant gVPLA$_2$ caused F-actin rearrangement to form gaps between ECs (*see arrows*) compared with ECs treated with vehicle only. Increased F-actin stress fibers and intercellular gaps were apparent within 5 minutes (Figure 6A), and persisted for at least 4 hours (Figure 6B). Coincubation with MCL-3G1 mAb against gVPLA$_2$ blocked the effects caused by gVPLA$_2$.

Because adherens junctions are the primary cell–cell connections regulating EC permeability, and are disrupted after LPS (26), the effect of recombinant gVPLA$_2$ on VE-cadherin distribution (the major adherens junction transcellular protein [7, 31]) within ECs also was determined at 5 minutes and at 4 hours (Figure 6). In ECs treated with vehicle alone, VE-cadherin formed thick, continuous bands at the intercellular regions surrounding ECs. In contrast, recombinant gVPLA$_2$ caused considerable disruption of these continuous VE-cadherin bands, with noticeable thinning within 5 minutes (Figure 6A). These effects were somewhat diminished at 4 hours, but were still persistent (Figure 6B). Coincubation with the specific MCL-3G1 mAb against gVPLA$_2$ attenuated these effects on F-actin and VE-cadherin disruption, whereas the control IgG had no effect. These data indicate that gVPLA$_2$ induces rapid and sustained F-actin rearrangement, junctional protein disruption, and intercellular gap formation, leading to increased EC permeability.

DISCUSSION

The objective of this investigation was to determine the role of the highly hydrolytic phospholipase, gVPLA$_2$, in mediating EC barrier disruption induced by LPS. We have reported previously that inhibition of gVPLA$_2$ by specific mAb or genetic deletion of gVPLA$_2$ blocked ALI caused by LPS in mice (19). Because those *in vivo* experiments did not allow for determination of the mechanistic sequence of events by which gVPLA$_2$ mediates ALI, we therefore explored these pathways in cell culture in the current study. To model *in vitro* the vascular permeability that occurs in ALI, we employed bacterial-derived LPS, a critical component in ALI caused by sepsis, and a well characterized agonist for disrupting EC barrier function *in vitro* (26, 32, 33).

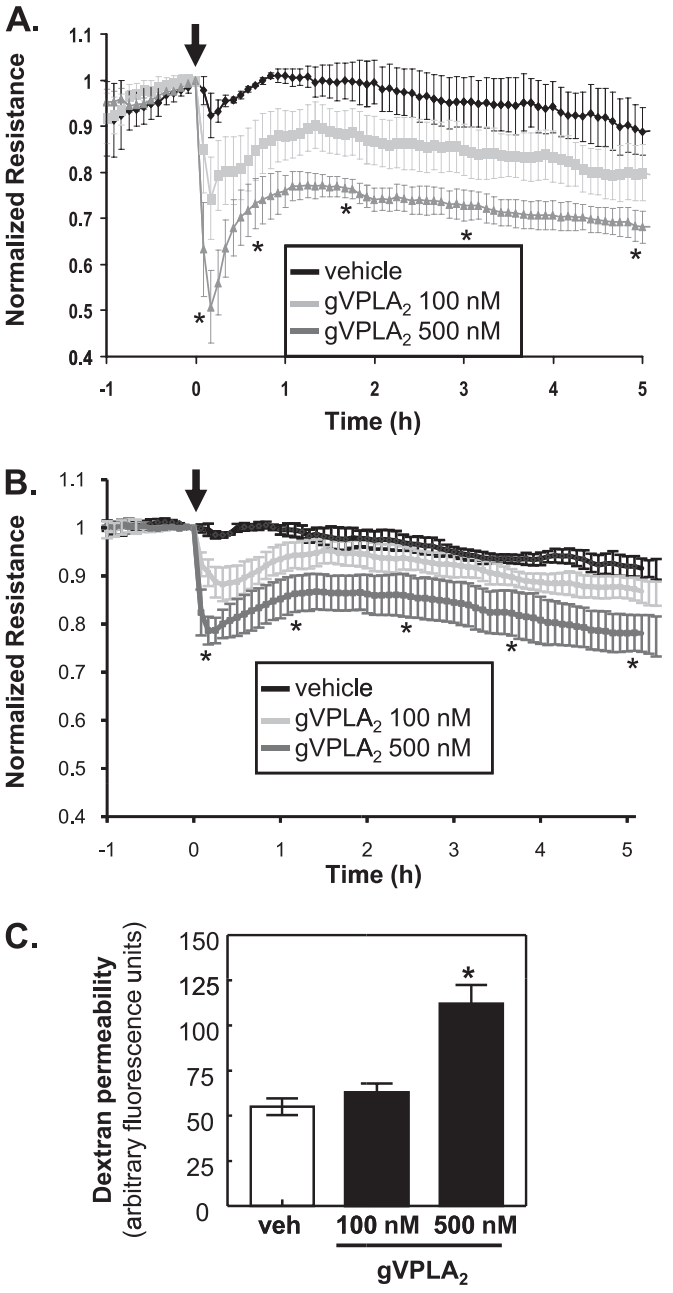

Figure 4. gVPLA$_2$ increases pulmonary EC permeability. HPAECs (*A*) or human lung microvascular ECs (HLMVECs) (*B*) were cultured on gold microelectrodes in serum free media and real-time TER measurements were taken as per Materials and Methods. At time 0 (*black arrow*), ECs were stimulated with recombinant gVPLA$_2$ (100 nM, *light gray line*; 500 nM, *dark gray line*) or vehicle control (*black line*). gVPLA$_2$ produced rapid and sustained disruption of EC barrier function in a dose-dependent fashion. Mean (±SE) shown for each time point ($n = 3$ per condition; $^*P < 0.05$ versus vehicle control at all time points). (*C*) Permeability to Dextran. HPAECs were cultured on polycarbonate filters as described in Materials and Methods, and then stimulated with 100 or 500 nM gVPLA$_2$ or vehicle. FITC-labeled dextran was added to the luminal compartment, and clearance across the EC monolayer was assayed after 2 hours by relative fluorescence excitation ($n = 3$ per condition; $^*P < 0.01$ versus all other conditions).

Our results indicate that human pulmonary ECs constitutively express gVPLA$_2$, that this expression (both mRNA and protein expression) was inducible by LPS within 4 hours, and

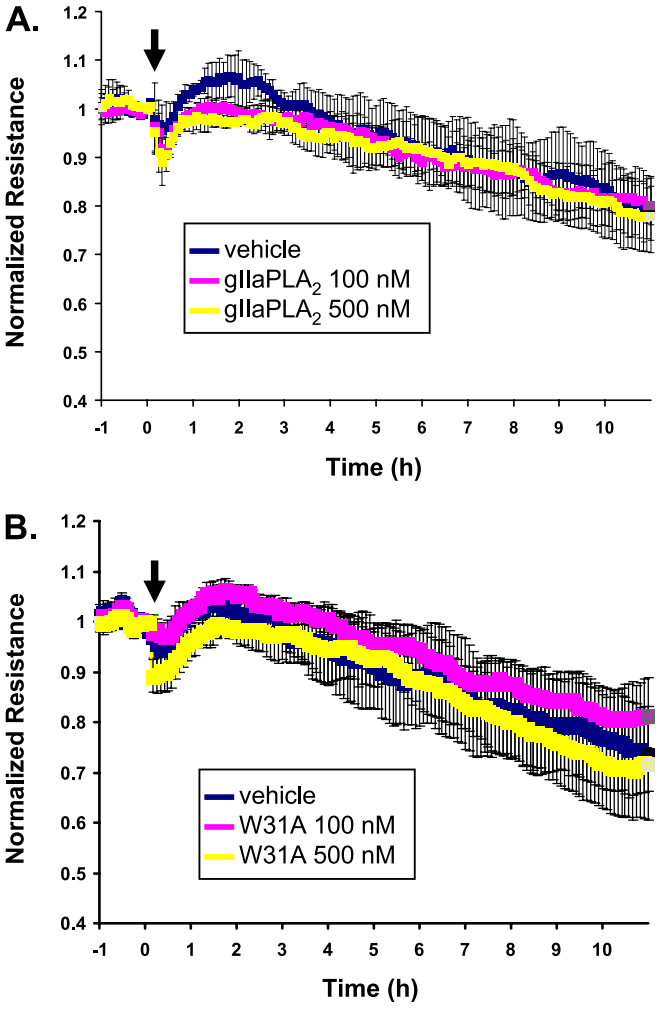

Figure 5. Increased EC permeability is specific to $gVPLA_2$. (*A*) Effect of $gIIaPLA_2$. At time 0, HPAECs were stimulated with recombinant $gIIaPLA_2$ (100 nM, *purple line*; 500 nM, *yellow*) or vehicle control (*dark blue*). Mean (±SE) shown for each time point ($n = 3$ per condition). (*B*) Effect of W31A $gVPLA_2$. At time 0 (*black arrow*), HPAECs were stimulated with recombinant W31A mutant $gVPLA_2$ (100 nM, *purple line*; 500 nM, *yellow line*) or vehicle control (*dark blue*). Means (±SE) shown for each time point ($n = 3$).

that $gVPLA_2$ was expressed at the outer membrane surface of pulmonary ECs in response to LPS (Figure 1). This increased expression of $gVPLA_2$ by ECs coincided temporally with disruption of EC barrier function by LPS, as measured by TER (Figure 2). Incubation with a specific mAb against $gVPLA_2$ blocked barrier disruption by LPS (Figure 2), as well as intercellular gap formation (Figure 3), suggesting a functional role for $gVPLA_2$ in mediating this effect.

Although prior work has revealed that $sPLA_2$ enzymes produce various eicosanoids that can affect EC permeability (34, 35), the specific effects of $gVPLA_2$ on EC barrier function have not been characterized previously. We found that recombinant $gVPLA_2$ caused sustained disruption of the EC barrier in a concentration-dependent manner in both macrovascular (Figure 4A) and microvascular (Figure 4B) pulmonary ECs. A Transwell assay using labeled dextran (~60 kD) determined that $gVPLA_2$ also increased EC permeability to larger particles (Figure 4C). This assay offers a more accurate approximation of the vascular protein (i.e., large molecule) flux that is a critical pathophysiologic component of ALI/ARDS syndromes. The effects of $gVPLA_2$ on EC permeability are specific to the $gVPLA_2$ enzyme, as the closely related 14-kD structural homolog, $gIIaPLA_2$, did not alter EC TER (Figure 5A). We also demonstrated that the phospholipase activity of $gVPLA_2$ is necessary to increase EC permeability, because the inactive mutant of $gVPLA_2$ (W31A) (29, 30) did not decrease TER (Figure 5B). These data suggest that $gVPLA_2$ causes pulmonary vascular leak in ALI through autocrine up-regulation and endogenous secretion of $gVPLA_2$ by lung ECs.

Although the precise mechanistic steps by which $gVPLA_2$ effects permeability changes on pulmonary ECs were not elucidated in the current study, one of two putative mechanisms may account for the development of EC barrier dysfunction caused by $gVPLA_2$. First, direct hydrolysis of the EC outer membrane by $gVPLA_2$ may physically disrupt its integrity to cause increased permeability. Alternatively, or in conjunction with direct membrane hydrolysis/disruption, the products of membrane hydrolysis generated by $gVPLA_2$ activity may initiate downstream signaling events that result in EC barrier dysfunction. $gVPLA_2$ produces multiple membrane hydrolysis products with potential biologic activity, including free fatty acid, arachidonic acid, lysophosphatidylcholine, lysophosphatidylethanolamine, lysophosphatidylserine, lysophosphatidylglycerol, lysophosphatidylinositol, and others (8, 36). Various eicosenoid mediators generated downstream of $gVPLA_2$ activity also have the potential to modulate EC barrier function (35). Detailed studies are ongoing to determine which of these numerous potential agents and mechanisms might be responsible for mediating increased EC permeability caused by $gVPLA_2$.

Previous studies in transgenic mice have established $gVPLA_2$ as pathophysiologically more relevant than its closely related 14-kD structural homolog, $gIIaPLA_2$, in lung injury syndromes (19, 37, 38). Although transgenic mice that overexpress $gIIaPLA_2$ exhibit no overt pulmonary abnormalities or inflammation (37), transgenic mice overexpressing $gVPLA_2$ die within several hours of birth due to respiratory failure that pathophysiologically resembles ALI (38). The lungs of these mice have extensive atelectasis, hyaline membrane formation in the airspaces, and thickened alveolar walls similar to the lungs of patients with ALI. Overexpression of the $gXPLA_2$ isoform of $sPLA_2$ in transgenic mice does not cause lung injury (38). Zymosan-induced plasma exudation is attenuated in $gVPLA_2$ knockout mice (20), suggesting a potential protective effect of $gVPLA_2$ deficiency during inflammation-induced vascular permeability. We have shown previously that $gVPLA_2$ knockout mice are protected from ALI caused by LPS (19). Thus, $gVPLA_2$ may be a critical target for modulation of the pathogenesis of ALI.

The current paradigm of EC barrier regulation suggests that a balance exists between cellular contractile forces and barrier-protective cell–cell and cell–matrix tethering forces (7). Both competing forces in this model are intimately linked to the actin-based endothelial cytoskeleton by a variety of actin-binding proteins, which are critical to both tensile force generation and linkage of the actin cytoskeleton to adhesive membrane components. This actin system is linked focally to multiple membrane adhesive proteins at sites of cell–cell (adherens junctions) and cell–matrix (focal adhesions) connections. Immunofluorescence studies demonstrated that $gVPLA_2$ rapidly caused rearrangement of EC F-actin, resulting in intercellular gap formation (Figure 6), which was blocked by coincubation with specific mAb against $gVPLA_2$ (MCL-3G1) (Figures 6). Recombinant $gVPLA_2$ also rapidly disrupted the normally continuous bands of VE-cadherin (the major adherens junction transcellular protein in ECs [7, 31]) that surround ECs. This process similarly was blocked by coincubation with specific

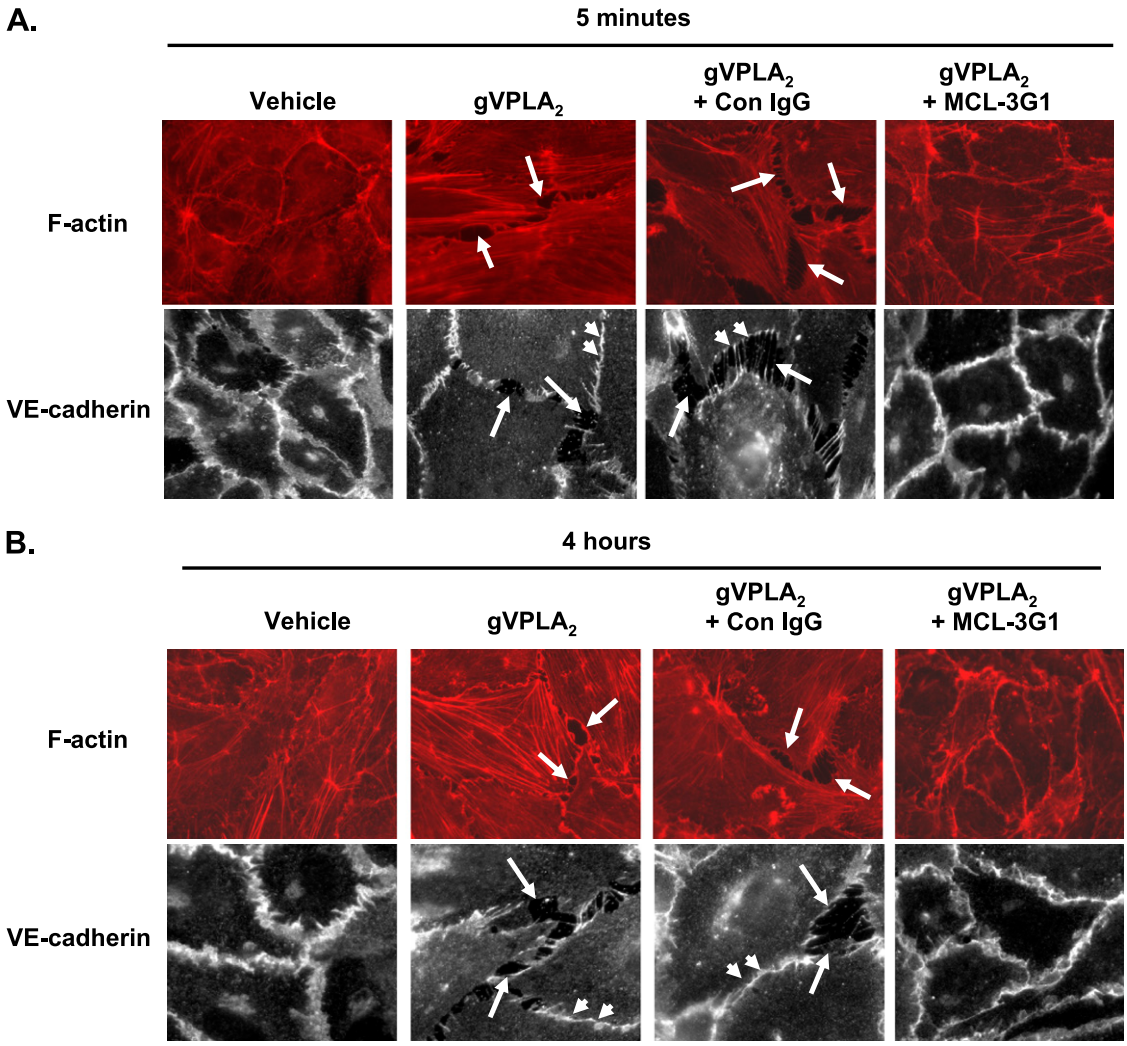

Figure 6. gVPLA$_2$ stimulates EC cytoskeletal rearrangement. HPAECs were incubated with vehicle or 500 nM recombinant gVPLA$_2$ for 5 minutes (*A*) or 4 hours (*B*), and stained for F-actin (*red*) or vascular endothelial (VE)–cadherin (*gray scale*), as described in MATERIALS AND METHODS. Parallel-treated cells were coincubated with 25 μg/ml MCL-3G1 mAb or 25 μg/ml IgG control Ab, as indicated. *Arrows* indicate intercellular gaps. *Arrowheads* indicate thinning of the intercellular VE-cadherin bands. *Images* are representative of three independent experiments.

mAb against gVPLA$_2$ (Figure 6). We conclude that gVPLA$_2$ causes vascular leak *in vitro* through activation of intercellular gap formation caused by F-actin and VE-cadherin rearrangement.

It is important to consider some limitations of our current findings. These data are derived exclusively from *in vitro* study. Because these studies were performed *in vitro* to obtain necessary stimulus isolation, these data cannot be extrapolated directly to the *in vivo* circumstance. We note, however, that these studies used human pulmonary ECs and recombinant human gVPLA$_2$, and, therefore, we believe that they may provide useful insights into how these processes occur in patients with ALI. Another potential limitation of this study is that the majority of our data is derived from observations using HPAECs, whereas, in ALI, pulmonary leak primarily occurs in the microvascular ECs of the alveolar–capillary interface (6). Others have reported differential properties of these two classes of ECs in terms of baseline barrier properties (39) and responses to various barrier-altering agonists, such as thapsigargin (27) or thrombin (28). However, in the current study, we demonstrate that gVPLA$_2$ disrupts HLMVEC permeability in a qualitatively similar manner as observed in HPAECs, although the magnitude of disruption was somewhat less in HLMVECs. These data suggest that our model provides useful insights into the effects of gVPLA$_2$ on human pulmonary EC permeability, despite the phenotypic limitations encountered when using cultured cells *in vitro*. It is also likely that other signaling molecules are responsible in mediating lung injury after LPS. Although ALI can be caused by multiple stimuli other than LPS (5), bacterial-derived LPS is a critical component in ALI caused by sepsis, and is a well characterized agonist for disrupting EC barrier function *in vitro* (26, 32, 33). Because sepsis is directly responsible for approximately 40% of ALI in humans (5), we chose LPS as the model for this initial characterization of the role of gVPLA$_2$ in ALI.

We conclude that gVPLA$_2$, which is constitutively expressed in human vascular ECs, is up-regulated in autocrine fashion by LPS. gVPLA$_2$ causes progressive and sustained increases in EC intercellular permeability, with associated leak of high–molecular weight molecules. Our studies thus provide preliminary evidence for a regulatory role for gVPLA$_2$ in the vascular leak of ALI.

Author Disclosure: None of the authors has a financial relationship with a commercial entity that has an interest in the subject of this manuscript.

Acknowledgments: The authors thank Joe G. N. Garcia for helpful discussions concerning this manuscript.

References

1. Rubenfeld GD, Caldwell E, Peabody E, Weaver J, Martin DP, Neff M, Stern EJ, Hudson LD. Incidence and outcomes of acute lung injury. *N Engl J Med* 2005;353:1685–1693.
2. The Acute Respiratory Distress Syndrome Network. Ventilation with lower tidal volumes as compared with traditional tidal volumes for acute lung injury and the acute respiratory distress syndrome. *N Engl J Med* 2000;342:1301–1308.

3. Erickson SE, Martin GS, Davis JL, Matthay MA, Eisner MD. Recent trends in acute lung injury mortality: 1996–2005. *Crit Care Med* 2009; 37:1574–1579.
4. Calfee CS, Matthay MA. Nonventilatory treatments for acute lung injury and ARDS. *Chest* 2007;131:913–920.
5. Wheeler AP, Bernard GR. Acute lung injury and the acute respiratory distress syndrome: a clinical review. *Lancet* 2007;369:1553–1564.
6. Maniatis NA, Kotanidou A, Catravas JD, Orfanos SE. Endothelial pathomechanisms in acute lung injury. *Vascul Pharmacol* 2008;49: 119–133.
7. Dudek SM, Garcia JG. Cytoskeletal regulation of pulmonary vascular permeability. *J Appl Physiol* 2001;91:1487–1500.
8. Boyanovsky BB, Webb NR. Biology of secretory phospholipase A_2. *Cardiovasc Drugs Ther* 2009;23:61–72.
9. Burke JE, Dennis EA. Phospholipase A_2 structure/function, mechanism, and signaling. *J Lipid Res* 2009;50:S237–S242.
10. Edelson JD, Vadas P, Villar J, Mullen JB, Pruzanski W. Acute lung injury induced by phospholipase A_2: structural and functional changes. *Am Rev Respir Dis* 1991;143:1102–1109.
11. Kaapa P, Soukka H. Phospholipase A_2 in meconium-induced lung injury. *J Perinatol* 2008;28:S120–S122.
12. Nakos G, Kitsiouli E, Hatzidaki E, Koulouras V, Touqui L, Lekka ME. Phospholipases A_2 and platelet-activating-factor acetylhydrolase in patients with acute respiratory distress syndrome. *Crit Care Med* 2005; 33:772–779.
13. Kim DK, Fukuda T, Thompson BT, Cockrill B, Hales C, Bonventre JV. Bronchoalveolar lavage fluid phospholipase A_2 activities are increased in human adult respiratory distress syndrome. *Am J Physiol* 1995;269:L109–L118.
14. Balestrieri B, Hsu VW, Gilbert H, Leslie CC, Han WK, Bonventre JV, Arm JP. Group V secretory phospholipase A_2 translocates to the phagosome after zymosan stimulation of mouse peritoneal macrophages and regulates phagocytosis. *J Biol Chem* 2006;281:6691–6698.
15. Wijewickrama GT, Kim JH, Kim YJ, Abraham A, Oh Y, Ananthanarayanan B, Kwatia M, Ackerman SJ, Cho W. Systematic evaluation of transcellular activities of secretory phospholipases A_2: high activity of group V phospholipases A_2 to induce eicosanoid biosynthesis in neighboring inflammatory cells. *J Biol Chem* 2006;281:10935–10944.
16. Muñoz NM, Boetticher E, Sperling AI, Kim KP, Meliton AY, Zhu X, Lambertino A, Cho W, Leff AR. Quantitation of secretory group V phospholipase A(2) in human tissues by sandwich enzyme-linked immunosorbent assay. *J Immunol Methods* 2002;262:41–51.
17. Muñoz NM, Kim KP, Han SK, Boetticher E, Sperling AI, Sano H, Zhu X, Cho W, Leff AR. Characterization of monoclonal antibodies specific for 14-kDa human group V secretory phospholipase A_2 ($hVPLA_2$). *Hybridoma* 2000;19:171–176.
18. Muñoz NM, Meliton AY, Lambertino A, Boetticher E, Learoyd J, Sultan F, Zhu X, Cho W, Leff AR. Transcellular secretion of group V phospholipase A_2 from epithelium induces beta 2-integrin–mediated adhesion and synthesis of leukotriene C4 in eosinophils. *J Immunol* 2006;177:574–582.
19. Muñoz NM, Meliton AY, Meliton LN, Dudek SM, Leff AR. Secretory group V phospholipase A_2 regulates acute lung injury and neutrophilic inflammation caused by LPS in mice. *Am J Physiol Lung Cell Mol Physiol* 2009;296:L879–L887.
20. Satake Y, Diaz BL, Balestrieri B, Lam BK, Kanaoka Y, Grusby MJ, Arm JP. Role of group V phospholipase A_2 in zymosan-induced eicosanoid generation and vascular permeability revealed by targeted gene disruption. *J Biol Chem* 2004;279:16488–16494.
21. Dudek SM, Jacobson JR, Chiang ET, Birukov KG, Wang P, Zhan X, Garcia JG. Pulmonary endothelial cell barrier enhancement by sphingosine 1-phosphate: roles for cortactin and myosin light chain kinase. *J Biol Chem* 2004;279:24692–24700.
22. Garcia JG, Liu F, Verin AD, Birukova A, Dechert MA, Gerthoffer WT, Bamberg JR, English D. Sphingosine 1-phosphate promotes endothelial cell barrier integrity by Edg-dependent cytoskeletal rearrangement. *J Clin Invest* 2001;108:689–701.
23. Camp SM, Bittman R, Chiang ET, Moreno-Vinasco L, Mirzapoiazova T, Sammani S, Lu X, Sun C, Harbeck M, Roe M, *et al.* Synthetic analogs of FTY720 [2-amino-2-(2-[4-octylphenyl]ethyl)-1,3-propanediol] differentially regulate pulmonary vascular permeability *in vivo* and *in vitro. J Pharmacol Exp Ther* 2009;331:54–64.
24. Gong P, Angelini DJ, Yang S, Xia G, Cross AS, Mann D, Bannerman DD, Vogel SN, Goldblum SE. TLR4 signaling is coupled to SRC family kinase activation, tyrosine phosphorylation of zonula adherens proteins, and opening of the paracellular pathway in human lung microvascular endothelia. *J Biol Chem* 2008;283:13437–13449.
25. Dudek SM, Camp SM, Chiang ET, Singleton PA, Usatyuk PV, Zhao Y, Natarajan V, Garcia JG. Pulmonary endothelial cell barrier enhancement by FTY720 does not require the S1P1 receptor. *Cell Signal* 2007; 19:1754–1764.
26. Schlegel N, Baumer Y, Drenckhahn D, Waschke J. Lipopolysaccharide-induced endothelial barrier breakdown is cyclic adenosine monophosphate dependent *in vivo* and *in vitro. Crit Care Med* 2009;37: 1735–1743.
27. Wu S, Cioffi EA, Alvarez D, Sayner SL, Chen H, Cioffi DL, King J, Creighton JR, Townsley M, Goodman SR, *et al.* Essential role of a Ca^{2+}-selective, store-operated current (ISOC) in endothelial cell permeability: determinants of the vascular leak site. *Circ Res* 2005;96: 856–863.
28. Troyanovsky B, Alvarez DF, King JA, Schaphorst KL. Thrombin enhances the barrier function of rat microvascular endothelium in a PAR-1–dependent manner. *Am J Physiol Lung Cell Mol Physiol* 2008;294:L266–L275.
29. Han SK, Kim KP, Koduri R, Bittova L, Muñoz NM, Leff AR, Wilton DC, Gelb MH, Cho W. Roles of Trp31 in high membrane binding and proinflammatory activity of human group V phospholipase A_2. *J Biol Chem* 1999;274:11881–11888.
30. Muñoz NM, Meliton AY, Arm JP, Bonventre JV, Cho W, Leff AR. Deletion of secretory group V phospholipase A_2 attenuates cell migration and airway hyperresponsiveness in immunosensitized mice. *J Immunol* 2007;179:4800–4807.
31. Vestweber D, Winderlich M, Cagna G, Nottebaum AF. Cell adhesion dynamics at endothelial junctions: VE-cadherin as a major player. *Trends Cell Biol* 2009;19:8–15.
32. Bannerman DD, Goldblum SE. Direct effects of endotoxin on the endothelium: barrier function and injury. *Lab Invest* 1999;79:1181–1199.
33. Bogatcheva NV, Zemskova MA, Kovalenkov Y, Poirier C, Verin AD. Molecular mechanisms mediating protective effect of cAMP on lipopolysaccharide (LPS)-induced human lung microvascular endothelial cells (HLMVEC) hyperpermeability. *J Cell Physiol* 2009;221:750–759.
34. Beck G, Yard BA, Schulte J, Haak M, van Ackern K, van der Woude FJ, Kaszkin M. Secreted phospholipases A_2 induce the expression of chemokines in microvascular endothelium. *Biochem Biophys Res Commun* 2003;300:731–737.
35. Bogatcheva NV, Sergeeva MG, Dudek SM, Verin AD. Arachidonic acid cascade in endothelial pathobiology. *Microvasc Res* 2005;69: 107–127.
36. Lambeau G, Gelb MH. Biochemistry and physiology of mammalian secreted phospholipases A_2. *Annu Rev Biochem* 2008;77:495–520.
37. Grass DS, Felkner RH, Chiang MY, Wallace RE, Nevalainen TJ, Bennett CF, Swanson ME. Expression of human group II PLA_2 in transgenic mice results in epidermal hyperplasia in the absence of inflammatory infiltrate. *J Clin Invest* 1996;97:2233–2241.
38. Ohtsuki M, Taketomi Y, Arata S, Masuda S, Ishikawa Y, Ishii T, Takanezawa Y, Aoki J, Arai H, Yamamoto K, *et al.* Transgenic expression of group V, but not group X, secreted phospholipase A_2 in mice leads to neonatal lethality because of lung dysfunction. *J Biol Chem* 2006;281:36420–36433.
39. Blum MS, Toninelli E, Anderson JM, Balda MS, Zhou J, O'Donnell L, Pardi R, Bender JR. Cytoskeletal rearrangement mediates human microvascular endothelial tight junction modulation by cytokines. *Am J Physiol* 1997;273:H286–H294.